

Cooperative Smartphone GNSS/PDR for Pedestrian Navigation

Changhui Jiang^{1b}, Yuwei Chen^{1b}, Chen Chen, Shoubin Chen^{1b}, Qian Meng^{1b}, Yuming Bo, and Juha Hyypä^{1b}

Abstract—Pedestrian navigation using smartphone built-in sensors attracted wide attention with the booming Location-based Service (LBS). Pedestrian Dead Reckoning (PDR) and Global Navigation Satellite System (GNSS) integration is recognized as a reliable solution for smartphone-based pedestrian navigation. However, GNSS is vulnerable under some conditions. Multi-path, None-Line-Of-Sight (NLOS), and signal blockage all pose negative impacts on GNSS position accuracy. PDR position errors increase with the pedestrian walking distance without GNSS. Aiming at improving the smartphone-based pedestrian position accuracy under GNSS signal challenging conditions, in this brief, we propose a cooperative PDR/GNSS integration method with Factor Graph Optimization (FGO). A factor graph is constructed to represent the relationship between the multiple agents' states, measurements and inter-ranging information. Optimal estimation is realized considering all the historical measurements and inter-ranging measurements between these agents. Field tests were carried out to assess the performance of the proposed cooperative navigation method. Results manifest that the proposed method can improve the position accuracy especially under the GNSS signals challenging conditions.

Index Terms—Smartphone, GNSS, PDR, pedestrian navigation, cooperative navigation.

Manuscript received 1 November 2022; accepted 10 December 2022. Date of publication 14 December 2022; date of current version 8 June 2023. This work was supported in part by the Academy of Finland Projects “Ultrafast Data Production With Broadband Photodetectors for Active Hyperspectral Space Imaging” under Grant 336145, Forest–Human–Machine Interplay—Building Resilience, Redefining Value Networks and Enabling Meaningful Experiences (UNITE) under Grant 337656, and Strategic Research Council Project Competence-Based Growth Through Integrated Disruptive Technologies of 3-D Digitalization, Robotics, Geospatial Information and Image Processing/Computing—Point Cloud Ecosystem under Grant 314312, and in part by Huawei under Grant 9424877. This brief was recommended by Associate Editor X. Ge. (*Corresponding author: Yuwei Chen.*)

Changhui Jiang, Chen Chen, and Juha Hyypä are with the Department of Photogrammetry and Remote Sensing, Finnish Geospatial Research Institute, 02430 Masala, Finland (e-mail: changhui.jiang@nls.fi; chen.chen@nls.fi; juha.hyypa@nls.fi).

Yuwei Chen is with the Department of Photogrammetry and Remote Sensing, Finnish Geospatial Research Institute, 02430 Masala, Finland, and also with the Laboratory of Advanced Laser Technology of Anhui Province, Hefei 230026, China (e-mail: yuwei.chen@nls.fi).

Shoubin Chen is with the School of Architecture and Urban Planning, Shenzhen University, Shenzhen 518060, China (e-mail: shoubin.chen@whu.edu.cn).

Qian Meng is with the School of Instrument Science and Engineering, Southeast University, Nanjing 210000, China (e-mail: qianmeng@seu.edu.cn).

Yuming Bo is with the School of Automation, Nanjing University of Science and Technology, Nanjing 210094, China (e-mail: byuming@njst.edu.cn).

Color versions of one or more figures in this article are available at <https://doi.org/10.1109/TCSII.2022.3229106>.

Digital Object Identifier 10.1109/TCSII.2022.3229106

I. INTRODUCTION

SMARTPHONE with various embedded sensors pose great impact on people's daily life. Smartphone-based location and position for pedestrian has been the research hotspot [1], [2]. Normally, a smartphone contains a chip-scale GNSS receiver, three-axis accelerometers and gyroscopes, barometer sensor, camera, magnetic sensor etc. Smartphone-based pedestrian position and navigation system is constructed via processing the measurements from the multiple sensors [3], [4]. In the outdoor environments, GNSS can provide position, navigation and timing (PNT) information under the condition that there are enough in-view satellites [5], [6]. However, GNSS signals are not always available under some signal challenging environments, i.e., indoors, city canyon, tunnels.

Pedestrian Dead Reckoning (PD) algorithm updates the pedestrian position with the estimated walking step and the heading angle [7]. However, the PDR position errors diverge over time due to the noises contained in the step length and heading angle. Therefore, PDR/GNSS integration as a more reliable solution is usually developed for smartphone-based pedestrian navigation. While GNSS is unavailable, standalone PDR can still work to generate position information.

Generally, PD/GNSS integration is constructed with the positions from the PDR and GNSS. However, GNSS is not always available [8], [9], [10]. How to improve the PDR accuracy without GNSS has attracted wide attention. Cooperative range information might be helpful to improve the PDR integration performance without GNSS. In addition, smartphone has other sensors, i.e., WIFI, Bluetooth, which can be utilized to acquire the ranging information between two different smartphones [3]. Ranging information has not been explored in aiding smartphone PDR under the GNSS denied environments. With the aim to improve the performance of PDR/GNSS integrated system, in this brief, we propose a cooperative PDR/GNSS integration method using a Factor Graph Optimization (FGO) algorithm. Ranging information between different smartphones are investigated to aid PDR under GNSS signal challenging environments. Different experiments were carried out to assess the performance of the proposed cooperative FGO-GNSS/PDR integration system. Contributions of this brief are summarized as:

(1) a cooperative PD/GNSS integration method with inter-ranging measurements constraints is proposed with the FGO method. An iterative solver is employed to find the optimal estimation of the states.

(2) feasibility of smartphone WI-Fi ranging measurements are investigated in the cooperative PDR/GNSS integration framework, its potentials to improve the PDR position accuracy under GNSS challenging environments are explored.

(3) we present a flexible cooperative PD/GNSS integration framework, which supports the agents and sensors integration in a “plug and play” manner. We open the source codes and expect this brief could inspire more exciting works on this topic.

Reminder of the brief is organized as: Section II presents cooperative FOG-GNSS/PDR method; Section III presents different experiments to assess the horizontal position errors of the proposed methods; Section IV points out the limitations and future works. Finally, conclusions are listed in Section V.

II. COOPERATIVE PD/GNSS INTEGRATION

In this section, firstly, the FOG-GNSS/PDR is introduced; secondly, the cooperative FGO-GNSS/PDR is described based on the FGO-GNSS/PDR.

A. FOG-GNSS/PDR

FOG-GNSS/PDR is described in our previous researches. Consecutive positions are correlated by the PDR position, the position increments between the two consecutive positions refers to the walking step stride length [11], [12]. The corresponding cost function is expressed as [11], [12]

$$\|\delta_{k+1}^{\text{PDR}}\|_{\Omega_{k+1}^{\text{PDR}}}^2 = \left\| \boldsymbol{\theta}_{k+1} - \left(\boldsymbol{\theta}_k + \begin{bmatrix} l_{k,k+1} \cdot \cos(\alpha_k) \\ l_{k,k+1} \cdot \sin(\alpha_k) \end{bmatrix} \right) \right\|_{\Omega_{k+1}^{\text{PDR}}}^2 \quad (1)$$

where $\delta_{k+1}^{\text{PDR}}$ means the cost, $\boldsymbol{\theta}$ denotes the PD position, l denotes the step length, α denotes the heading angle, $\Omega_{k+1}^{\text{PDR}}$ refers to the corresponding covariance matrix.

In addition, at each step, GNUS position measurements restrict the state. The GNSS factor cost function is expressed as

$$\|\delta_{k+1}^{\text{GNSS}}\|_{\Omega_{k+1}^{\text{GNSS}}}^2 = \left\| \boldsymbol{\theta}_{k+1} - \boldsymbol{\theta}_{k+1}^{\text{GNSS}} \right\|_{\Omega_{k+1}^{\text{GNSS}}}^2 \quad (2)$$

where $\delta_{k+1}^{\text{GNSS}}$ denotes the GNUS factor cost at the $k+1$ epoch, the $\Omega_{k+1}^{\text{GNSS}}$ denotes the corresponding covariance matrix.

At each step, the state optimal estimation is solved by minimizing the cost function, which is expressed as

$$\boldsymbol{\theta}_{k+1}^* = \operatorname{argmin} \left(\left\| \delta_{k+1}^{\text{PDR}} \right\|_{\Omega_{k+1}^{\text{PDR}}}^2 + \left\| \delta_{k+1}^{\text{GNSS}} \right\|_{\Omega_{k+1}^{\text{GNSS}}}^2 \right) \quad (3)$$

where $\operatorname{argmin}(\cdot)$ denotes the function minimizing the costs.

As expressed in the equation (3), the positions are time-correlated. Specifically, the consecutive positions are correlated. In addition, we can observe that, in the equations (3-5), both the $\boldsymbol{\theta}_{k+1}$ and $\boldsymbol{\theta}_k$ are unknown, optimal estimates of these states are expected while regarding all the past states as unknowns. Assuming a set of states $\boldsymbol{\theta} = (\boldsymbol{\theta}_1, \boldsymbol{\theta}_2, \dots, \boldsymbol{\theta}_{k+1})$, and the optimal estimates can be expressed as

$$\begin{aligned} \boldsymbol{\theta}^* &= (\boldsymbol{\theta}_1^*, \boldsymbol{\theta}_2^*, \dots, \boldsymbol{\theta}_{k+1}^*) \\ &= \operatorname{argmin} \left(\sum_{i=1}^k \left(\left\| \delta_{i+1}^{\text{PDR}} \right\|_{\Omega_{i+1}^{\text{PDR}}}^2 + \left\| \delta_{i+1}^{\text{GNSS}} \right\|_{\Omega_{i+1}^{\text{GNSS}}}^2 \right) \right) \quad (4) \end{aligned}$$

where the Gauss-Newton or Ehrenberg-Marquardt methods can obtain the optimal estimates based on the rule minimizing the costs [12], [13], [14].

Since the heading angle and the misalignment angle between the smartphone and the walking direction affect the position updating in the PDR, the step stride length can be



Fig. 1. Connections between different pedestrian smartphones.

directly utilized in the PDR/GNSS integration. Cost function utilizing the step stride length is expressed as

$$\|\delta_{k+1}^{\text{SSL}}\|_{\Omega_{k+1}^{\text{SSL}}}^2 = \left\| l_{k,k+1} - \|\boldsymbol{\theta}_{k+1} - \boldsymbol{\theta}_k\| \right\|_{\Omega_{k+1}^{\text{SSL}}}^2 \quad (5)$$

where $\delta_{k+1}^{\text{SSL}}$ means the cost, $\|\boldsymbol{\theta}_{k+1} - \boldsymbol{\theta}_k\|$ means the distance between two consecutive positions. Similarly, the optimal estimates of the states are expressed as

$$\begin{aligned} \boldsymbol{\theta}^* &= (\boldsymbol{\theta}_1^*, \boldsymbol{\theta}_2^*, \dots, \boldsymbol{\theta}_{k+1}^*) \\ &= \operatorname{argmin} \left(\sum_{i=1}^k \left(\left\| \delta_{i+1}^{\text{SSL}} \right\|_{\Omega_{i+1}^{\text{SSL}}}^2 + \left\| \delta_{i+1}^{\text{GNSS}} \right\|_{\Omega_{i+1}^{\text{GNSS}}}^2 \right) \right) \quad (6) \end{aligned}$$

where the Gauss-Newton or Ehrenberg-Marquardt methods can be utilized to find the optimal estimates via minimizing the cost values. Compared with the equation (4), the $\delta_{i+1}^{\text{SSL}}$ are nonlinear with the respect to the position.

B. Cooperative GNUS/PDR

Previous subsection presents two different FOG-PDR/GNSS integration models for single-agent pedestrian navigation. In fact, different smartphones can be connected via Wi-Fi, personal hotspot or possible UWB [4], [5]. Measurements, i.e., distance, angle of arrival, can be extracted from the connection. Therefore, cooperative navigation system can be constructed with different smartphones. Fig. 1 presents an illustrative example describing the relationship between the smartphones. When the range measurements between different smartphones are available, the cooperative PDR/GNSS integration system can be built with the distance connections. Two different cooperative navigation methods are presented in this section based on the GNSS/PDR integration models in previous subsection. For explicitly presenting how the cooperative navigation system estimate the navigation information, we employ a three-agent cooperative navigation framework to illustrating the mechanism. In addition, adding more agents to the cooperative navigation system is also feasible with the FGO-PDR/GNSS integration framework.

Compared with the single-agent GNUS/PDR integration, inter-range factors between the states from different agents are added to the graph. Fig. 2 presents the factor graph for the cooperative GNSS/PDR integration. Compared with the equation (4), ranging factors are added to the cost function. Therefore, the cost function of the three-agent cooperative

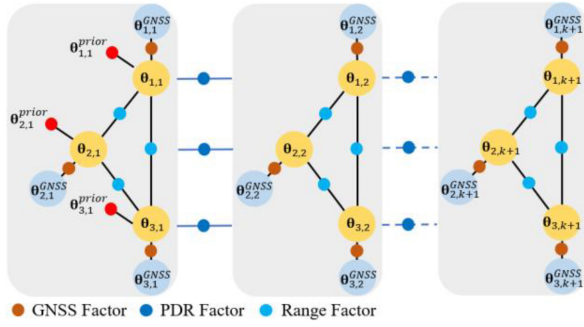


Fig. 2. Cooperative PD/GNSS integration with three agents.

PDR/GNSS integration is expressed as

$$\theta^* = \arg \min \left\{ \sum_{j=1}^3 \left(\sum_{i=1}^k \left(\|\delta_{j,i+1}^{\text{PDR}}\|_{\Omega_{j,i+1}^{\text{PDR}}}^2 + \|\delta_{j,i+1}^{\text{GNSS}}\|_{\Omega_{j,i+1}^{\text{GNSS}}}^2 \right) \right) + \sum_{i=1}^{k+1} \left(\|\mathbf{D}_i^{12}\|_{\Omega_i^D}^2 \right) + \sum_{i=1}^{k+1} \left(\|\mathbf{D}_i^{13}\|_{\Omega_i^D}^2 \right) + \sum_{i=1}^{k+1} \left(\|\mathbf{D}_i^{23}\|_{\Omega_i^D}^2 \right) \right\} \quad (7)$$

where θ^* denotes a set of state variables, and its specifications are expressed as

$$\theta^* = \left((\theta_{1,1}, \theta_{1,2}, \dots, \theta_{1,k+1})^*, (\theta_{2,1}, \theta_{2,2}, \dots, \theta_{2,k+1})^*, (\theta_{3,1}, \theta_{3,2}, \dots, \theta_{3,k+1})^* \right) \quad (8)$$

$$\|\delta_{j,i+1}^{\text{PDR}}\|_{\Omega_{j,i+1}^{\text{PDR}}}^2 = \left\| \theta_{j,k+1} - \left(\theta_{j,k} + \begin{bmatrix} l_{k,k+1}^j \cdot \cos(\alpha_k^j) \\ l_{k,k+1}^j \cdot \sin(\alpha_k^j) \end{bmatrix} \right) \right\|_{\Omega_{j,i+1}^{\text{PDR}}}^2 \quad (9)$$

$$\|\delta_{j,i+1}^{\text{GNSS}}\|_{\Omega_{j,i+1}^{\text{GNSS}}}^2 = \left\| \theta_{j,k+1} - \theta_{j,k+1}^{\text{GNSS}} \right\|_{\Omega_{j,i+1}^{\text{GNSS}}}^2 \quad (10)$$

\mathbf{D}_i^{12} , \mathbf{D}_i^{13} and \mathbf{D}_i^{23} denote the ranges between the three agents for i step, and they are expressed as

$$\mathbf{D}_i^{12} = \left\| \mathbf{d}_i^{12} - \|\theta_{1,i} - \theta_{2,i}\| \right\| \quad (11)$$

$$\mathbf{D}_i^{13} = \left\| \mathbf{d}_i^{13} - \|\theta_{1,i} - \theta_{3,i}\| \right\| \quad (12)$$

$$\mathbf{D}_i^{23} = \left\| \mathbf{d}_i^{23} - \|\theta_{2,i} - \theta_{3,i}\| \right\| \quad (13)$$

In addition, a new model which directly utilizing the step length in the PD/GNSS integration with cooperative agents is constructed.

$$\theta^* = \arg \min \left\{ \sum_{j=1}^3 \left(\sum_{i=1}^k \left(\|\delta_{j,i+1}^{\text{SSL}}\|_{\Omega_{j,i+1}^{\text{SSL}}}^2 + \|\delta_{j,i+1}^{\text{GNSS}}\|_{\Omega_{j,i+1}^{\text{GNSS}}}^2 \right) \right) + \sum_{i=1}^{k+1} \left(\|\mathbf{D}_i^{12}\|_{\Omega_i^D}^2 \right) + \sum_{i=1}^{k+1} \left(\|\mathbf{D}_i^{13}\|_{\Omega_i^D}^2 \right) + \sum_{i=1}^{k+1} \left(\|\mathbf{D}_i^{23}\|_{\Omega_i^D}^2 \right) \right\} \quad (14)$$

where

$$\|\delta_{j,i+1}^{\text{SSL}}\|_{\Omega_{j,i+1}^{\text{SSL}}}^2 = \left\| l_{k,k+1}^j - \|\theta_{j,k+1} - \theta_{j,k}\| \right\|_{\Omega_{j,i+1}^{\text{SSL}}}^2 \quad (15)$$

$\|\delta_{j,i+1}^{\text{GNSS}}\|_{\Omega_{j,i+1}^{\text{GNSS}}}^2$, \mathbf{D}_i^{12} , \mathbf{D}_i^{13} and \mathbf{D}_i^{23} are the same as that listed in the equations (11)-(13). Different from equation (7), the model in the equation (14) utilizing the step length instead of position in the integration, which can alleviate the negative influence of the heading angle on the position errors.

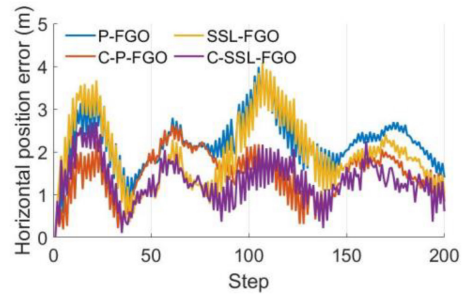


Fig. 3. Horizontal position errors comparison for Agent01.

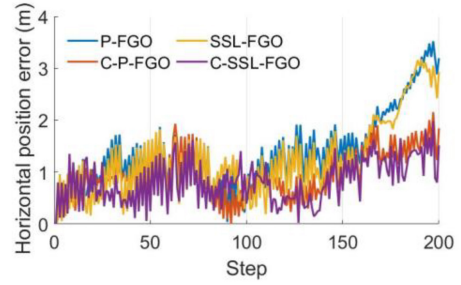


Fig. 4. Horizontal position errors comparison.

After constructing the cost function, Ehrenberg-Marquardt (LM) or Dogleg trust-region method is usually employed to solve for the optimal estimations. We utilize the Georgia Tech Smoothing and Mapping (GTSAM) library to implement the FGO-GNSS/PDR and cooperative GNSS/PDR [11], [12], [13], [14], [15].

III. EXPERIMENTS AND RESULTS

With the aim to evaluate the performance of the proposed methods, field experiments were carried out with two different smartphones. Sensors' datasets were collected for analysis. A commercial product Nova tel SPAN-CPT was employed as the trajectory reference to calculate the position errors, and the equipment is installed in the backpack box.

A. Backpack Smartphone Experiments

In the first filed test, we installed a smartphone horizontally on a backpack box for assessing the advances on the position accuracy brought by the multi-agent cooperation. Before introducing the experimental results, we name the methods presented in Section III. PD/GNSS integration method with position is named as P-FGO; PDR/GNSS integration with step stride length is named as SSL-FGO; the cooperative PDR/GNSS integration with position is named as C-P-FGO; and the cooperative PDR/GNSS integration with step stride length is named as C-SSL-FGO. In the experiment, for saving the hardware, following assumptions are defined before the experimental results.

(1) A reference trajectory from the SPAN-PCT is presented in the Fig. 5, we divide the trajectory into three parts to simulate three different agents. Corresponding measurements from the smartphone are processed individually.

(2) Ranging measurements between the agents are calculated via adding Gaussian noises to the trajectory reference.

Following Fig. 6, Fig. 7 and Fig. 8 present the horizontal position errors for the three agents with above four methods.

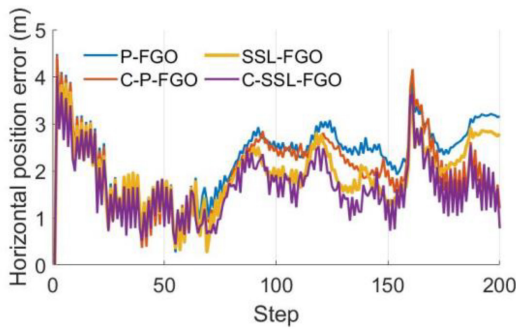


Fig. 5. Horizontal position errors comparison.

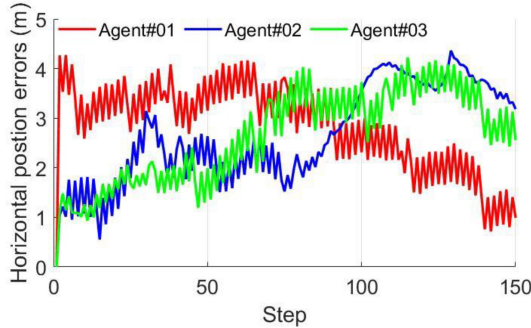


Fig. 6. Horizontal position errors with GNUS.

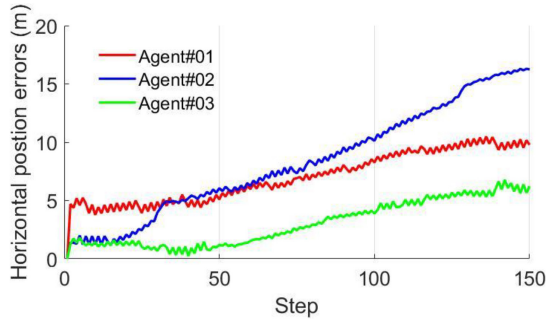


Fig. 7. Horizontal position errors without GNUS.

Specifically. It can be seen that (1) the ISL-FGO and C-SSL-FGO methods perform better than P-FGO and C-P-FGO individually, direct utilization of step stride length obtains better performance in optimizing the position estimation; (2) the C-P-FGO and C-SSL-FGO methods are both effective to reduce the position errors compared with that from the P-FGO and SSL-FGO methods, cooperative ranging constraints are effective to improve the position estimation through the FGO method.

Statistical analysis results are listed in the Table I, mean values and the standard deviation values of the horizontal position errors are calculated for qualitatively comparing the performance of the different methods. In aspects of the Agent01, the mean values of the horizontal position errors from the C-P-FGO and C-SSL-FGO methods reduce by 32.6% and 32.3% compared with the P-FGO and SSL-FGO methods individually; for the Agent#02, the corresponding mean values obtain 29.9% and 33.3% reduction while adding the inter-ranging measurements as the constraints in optimizing the position estimation; for the Agent#03, similar improvements of the horizontal position errors are also observed, the

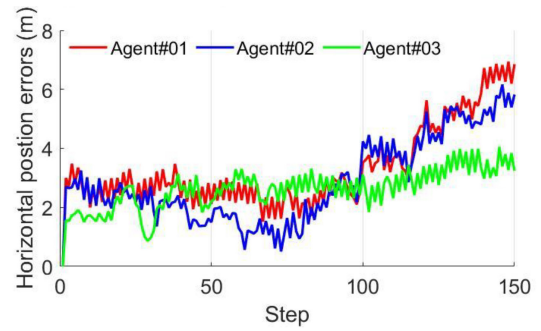


Fig. 8. Cooperative PD horizontal position errors without GNSS.

TABLE I
STATISTICAL ANALYSIS

Method	Agent#01		Agent#02		Agent#03	
	Mean	STD	Mean	STD	Mean	STD
P-FGO	2.21	0.66	1.37	0.74	2.29	0.78
C-P-FGO	1.49	0.55	0.96	0.47	2.02	0.77
SSL-FGO	1.95	0.80	1.23	0.74	1.93	0.70
C-SSL-FGO	1.32	0.52	0.82	0.42	1.66	0.68

mean values of the C-P-FGO horizontal position errors reduce by 11.8% compared with that from the P-FGO, and the C-SSL-FGO gains 14.0% in terms of the mean values of the horizontal position errors.

B. Cooperative PD With Partial GNSS Outages

After assessing the performance under ideal GNUS environments, we collected another dataset with handheld smartphone for evaluating the cooperative PDR method under GNSS signal challenging environments. Similar to that presented in the previous subsection, we divide the trajectory into three parts to simulate three agents. Fig. 6 presents the individual PDR/GNSS integration results with the P-FGO method, and horizontal position errors are below 4.5 meters. Fig. 7 shows the PDR results without GNSS. It can be observed that the horizontal position results diverge over time without GNSS. Fig. 8 presents the horizontal position errors adding the inter-ranging measurements to the cooperative PDR via FGO. The maximum values of the horizontal position errors from the agents decrease at different degrees. Especially for the Agent#02, its maximum horizontal position errors decrease from approximately 17 meters to 6 meters. The cooperative ranging measurements are effective to reduce the horizontal position errors even if the GNSS is not available.

In addition, we assess the cooperative PD/GNSS under the condition that the GNSS signals of the part of the agents is unavailable. Fig. 9 shows the horizontal position errors while the Agent#01 has no GNSS. It can be seen that the Agent#01 horizontal position errors do not diverge over time, which demonstrates the cooperative ranging measurements are effective to reduce the agent#01 horizontal position errors.

C. Wi-Fi Ranging Aided Cooperative PDR

Since smartphone has Wi-Fi module, we carried out tests with Wi-Fi measuring the range information. Specifically, a Huawei P40 Lite and Mate 40 Pro were utilized to collect the datasets. In the first experiment, the Mate 40 Pro keeps static, and the Huawei P40 Lite works around the Mate 40 Pro. In

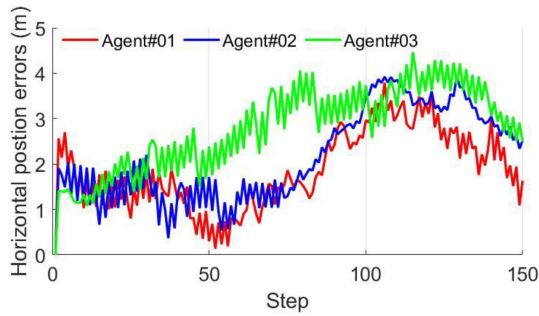


Fig. 9. Cooperative PD/GNSS integration while no GNSS for Agent#01.

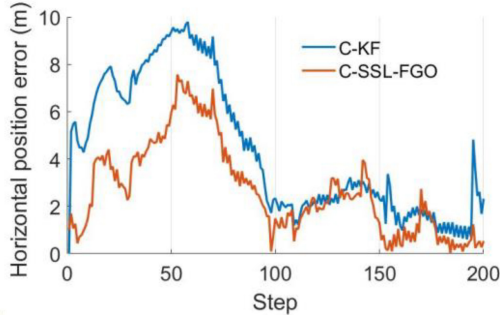


Fig. 10. Horizontal position results comparison.

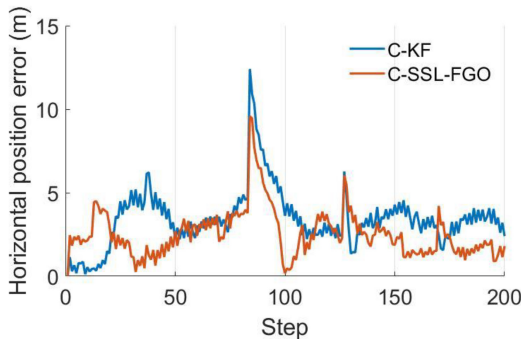


Fig. 11. Horizontal position results comparison.

the second experiment, Huawei P40 Lite walks followed by Mate 40 Pro. P40 Lite is connected to Mate 40 Pro Wi-Fi hotspot, and the range information is extracted through the Wi-Fi signal strength.

Fig. 10 and Fig. 11 present the horizontal position results from the two experiments. The legend “C-KPH” refers to the method KF based cooperative GNSS/PDR described in Section II. It can be observed that C-SSL-FGO performs better than C-KF. Mean values of the position results from C-SSL-FGO reduce by 38.6% and 25.9% for the two experiments respectively.

IV. DISCUSSIONS AND LIMITATIONS

Although the experimental results support that the proposed method can improve the position accuracy, following works are expected.

(1) how to acquire the ranging information more efficiently is the key to construct the cooperative navigation system, which is of great significance.

(2) FOG method requires much more computation than KF, it is of great importance to reduce the computation cost while keeping the performance.

V. CONCLUSION

In this brief, we investigated the FOG based smartphone cooperative PDR/GNSS integration. With the experimental results, following conclusions are draw: (1) cooperative PDR/GNSS integration can obtain superior horizontal position results compared with the individual results; (2) direct utilization of the step stride length in the FGO-PDR/GNSS integration contributes to better horizontal position estimation results; (3) FGO can improve the cooperative GNSS/PDR compared with KF.

ACKNOWLEDGMENT

The authors appreciate the open-source PD code [17].

REFERENCES

- [1] T. Lou, X. Niu, J. Kuang, S. Cao, L. Zhang, and X. Chen, “Doppler shift mitigation in acoustic positioning based on pedestrian dead reckoning for smartphone,” *IEEE Trans. Instrum. Meas.*, vol. 70, pp. 1–11, Jul. 2020.
- [2] S. Schiaparelli et al., “Single IMU displacement and orientation estimation of human center of mass: A magnetometer-free approach,” *IEEE Trans. Instrum. Meas.*, vol. 69, no. 8, pp. 5629–5639, Aug. 2020.
- [3] S. IUD et al., “Multi-sensor information fusion based on machine learning for real applications in human activity recognition: State-of-the-art and research challenges,” *Inf. Fusion*, vol. 80, pp. 241–265, Apr. 2022.
- [4] Z. Chen, Q. Thu, and Y. C. Soh, “Smartphone inertial sensor-based indoor localization and tracking with i Beacon corrections,” *IEEE Trans. Ind. Informat.*, vol. 12, no. 4, pp. 1540–1549, Aug. 2016.
- [5] W. Sellout, A. Latoui, R. Canals, A. Chetouani, and S. Treuillet, “Indoor pedestrian localization with a smartphone: A comparison of inertial and vision-based methods,” *IEEE Sensors J.*, vol. 16, no. 13, pp. 5376–5388, Jul. 2016.
- [6] H. S. Mahdi, I. A. Lami, K. Z. Ghafoor, and J. Lloret, “Seamless outdoors-indoors localization solutions on smartphones: Implementation and challenges,” *CAM Comput. Surv.*, vol. 48, no. 4, pp. 1–34, 2016.
- [7] T. T. Pam and Y. S. Suh, “Conditional generative adversarial network-based regression approach for walking distance estimation using waist-mounted inertial sensors,” *IEEE Trans. Instrum. Meas.*, vol. 71, May 2022, Art. no. 2510113.
- [8] B. Thou, Q. Li, Q. Mao, W. Tu, and X. Zhang, “Activity sequence-based indoor pedestrian localization using smartphones,” *IEEE Trans. Human-Mach. Syst.*, vol. 45, no. 5, pp. 562–574, Oct. 2015.
- [9] L.-T. Hus, Y. Gu, Y. Huang, and S. Kamijo, “Urban pedestrian navigation using smartphone-based dead reckoning and 3-D map-aided GNUS,” *IEEE Sensors J.*, vol. 16, no. 5, pp. 1281–1293, Mar. 2016.
- [10] D. Xe et al., “A robust GNUS/PDR integration scheme with GRU-based zero-velocity detection for mass-pedestrians,” *Remote Sens.*, vol. 14, no. 2, p. 300, 2022.
- [11] C. Jiangxi et al., “Smartphone PDR/GNSS integration via factor graph optimization for pedestrian navigation,” *IEEE Trans. Instrum. Meas.*, vol. 71, Jun. 2022, Art. no. 8504112.
- [12] C. Jiangxi et al., “Implementation and performance analysis of the PD/GNSS integration on a smartphone,” *GPS Solutions*, vol. 26, no. 3, pp. 1–9, 2022.
- [13] C. Jiangxi, S. Chen, Y. Chen, D. Liu, and Y. Bo, “GNUS vector tracking method using graph optimization,” *IEEE Trans. Circuits Syst. II, Exp. Briefs*, vol. 68, no. 4, pp. 1313–1317, Apr. 2021.
- [14] T. Suzuki, “Time-relative RT-GNSS: GNSS loop closure in pose graph optimization,” *IEEE Robot. Autom. Lett.*, vol. 5, no. 3, pp. 4735–4742, Jul. 2020.
- [15] C. Jiangxi, S. Chen, Y. Chen, J. Shen, D. Liu, and Y. Bo, “Superior position estimation based on optimization in GNUS,” *IEEE Commun. Lett.*, vol. 25, no. 2, pp. 479–483, Feb. 2021.
- [16] Y. Li, Y. Huang, H. Lan, P. Zhang, X. Niu, and N. El-Sheimy, “Self-contained indoor pedestrian navigation using smartphone sensors and magnetic features,” *IEEE Sensors J.*, vol. 16, no. 19, pp. 7173–7182, Oct. 2016.
- [17] [Online]. Available: <http://lopsi.weebly.com/downloads.html>